

Non-perturbative improvement and renormalization of the axial current in $N_f = 3$ lattice QCD



MS-TP-15-04

John Bulava

School of Mathematics, Trinity College, Dublin 2, Ireland

E-mail: jbulava@maths.tcd.ie

Michele Della Morte

CP³-Origins & Danish IAS, University of Southern Denmark,

Campusvej 55, 5230 Odense M, Denmark

E-mail: dellamor@cp3-origins.net

Jochen Heitger*

University of Münster, Wilhelm-Klemm-Straße 9, 48149 Münster, Germany

E-mail: heitger@uni-muenster.de

Christian Wittemeier*

University of Münster, Wilhelm-Klemm-Straße 9, 48149 Münster, Germany

E-mail: christian.wittemeier@uni-muenster.de

We report on a non-perturbative computation of the renormalization factor Z_A of the axial vector current in three-flavour $O(a)$ improved lattice QCD with Wilson quarks and tree-level Symanzik improved gauge action and also recall our recent determination of the improvement coefficient c_A . Our normalization and improvement conditions are formulated at constant physics in a Schrödinger functional setup. The normalization condition exploits the full, massive axial Ward identity to reduce finite quark mass effects in the evaluation of Z_A and correlators with boundary wave functions to suppress excited state contributions in the pseudoscalar channel.

The 32nd International Symposium on Lattice Field Theory

23-28 June, 2014

Columbia University New York, NY

*Speaker.

1. Introduction

Wilson fermions [1] are a popular way of discretizing fermions in lattice QCD. Their main drawback is that they break chiral symmetry. As a consequence, they are afflicted with discretization errors linear in the lattice spacing a . These $O(a)$ errors can be removed by adding the Sheikholeslami-Wohlert term (clover term) to the Wilson action [2] and further improvement terms to the matrix elements of interest. This method of $O(a)$ improvement has become known as ‘Symanzik improvement program’ [3, 4]. Moreover, currents which are conserved in a chiral theory and hence need not be renormalized require a finite renormalization with Wilson fermions. One of these currents is the isovector axial current which we are concerned with in this work.

The isovector axial current is a quark bilinear and in its bare form it can be written as

$$A_\mu^a(x) = \bar{\psi}(x) \gamma_\mu \gamma_5 \frac{\tau^a}{2} \psi(x), \quad (1.1)$$

where τ^a is a matrix acting in flavor space. Symanzik’s effective theory predicts that the axial current will mix with the derivative of the pseudoscalar density $P^a(x)$ at $O(a)$, when the lattice discretization breaks chiral symmetry. This can be compensated for by adding a corresponding improvement term to the bare current. Its coefficient is denoted by c_A and is at the heart of improving the axial current.

Furthermore, the axial current is renormalized by multiplying it by the renormalization factor Z_A and another mass-dependent term. Thus, the fully renormalized and improved axial current on the lattice is

$$(A_R)_\mu^a(x) = Z_A (1 + b_A am_q) [A_\mu^a(x) + a c_A \partial_\mu P^a(x)] \quad \text{with} \quad P^a(x) = \bar{\psi}(x) \gamma_5 \frac{\tau^a}{2} \psi(x). \quad (1.2)$$

The axial current plays a fundamental rôle in many applications, notably the computation of quark masses and meson decay constants in the pseudoscalar sector. These are not only of phenomenological interest, but they provide a precise way of setting a physical scale in lattice simulations, too. One observable that can be used for this purpose is the kaon decay constant f_K [5]. In these contexts, it is crucial to employ the improved and renormalized current, since, typically, improvement and renormalization each contribute about 10-20% to the final result [6, 7, 8]. Both can be computed in perturbation theory. However, in previous works it was found that the non-perturbative results deviate strongly from the 1-loop estimates. The deviations can be several times the 1-loop contribution itself. Therefore, it is desirable to determine c_A and Z_A in a non-perturbative way.

The methods we use to determine c_A and Z_A have been introduced in previous papers, which applied them to the quenched [9, 10] and two-flavor QCD cases [6, 8]. Here, we look at an action with $O(a)$ improved $N_f = 3$ mass-degenerate dynamical Wilson fermions [11] and the tree-level Symanzik-improved gauge action (TLI gauge action) [12]. The main part of this text is about the renormalization of the axial current. The renormalization condition is summarized in section 2, the ensembles of gauge field configurations that we used are described in section 3, and our preliminary results, in particular for the interpolating function for Z_A (valid for lattice spacings $\lesssim 0.09$ fm), can be found in section 4. The determination of the improvement coefficient c_A was recently finished and will be published soon [13]. We will only reproduce the main result in section 4. A preliminary report can also be found in [14].

2. Renormalization Condition

Renormalization conditions for the axial current are based on the idea that they can restore chiral Ward identities, which are broken by the Wilson term, up to $O(a^2)$. This is done by choosing one particular Ward identity and adjusting Z_A so that it holds exactly. The condition that we choose has been introduced for simulations with two dynamical fermions [8], but a similar condition has already been used in the quenched case [10]. We give a shortened description of its derivation below. More details can be found in the original papers.

The Ward identity our renormalization condition is based on is similar to the PCAC relation, i.e., it is derived from a chiral rotation of the quark fields, but, in addition, the axial current $A_V^b(y)$ is inserted as an internal operator. The resultant identity is

$$\int_{\partial R} d\sigma_\mu(x) \langle A_\mu^a(x) A_V^b(y) \mathcal{O}_{\text{ext}} \rangle - 2m \int_R d^4x \langle P^a(x) A_V^b(y) \mathcal{O}_{\text{ext}} \rangle = i\epsilon^{abc} \langle V_V^c(y) \mathcal{O}_{\text{ext}} \rangle, \quad (2.1)$$

where R is an arbitrary region containing y , \mathcal{O}_{ext} is an operator built from fields outside R , and V_V^c is the isovector vector current. As region R we choose the spacetime volume between two space-like hyperplanes. Furthermore, eq. (2.1) can be modified by using the PCAC relation to shift the integration domains. Setting $v = 0$ and contracting the flavor indices a and b with ϵ^{abc} , one arrives at

$$\begin{aligned} \int d^3\mathbf{x} d^3\mathbf{y} \epsilon^{abc} \langle A_0^a(x) A_0^b(y) \mathcal{O}_{\text{ext}} \rangle \\ - 2m \int d^3\mathbf{x} d^3\mathbf{y} \int_{y_0}^{x_0} dx_0 \epsilon^{abc} \langle P^a(x) A_0^b(y) \mathcal{O}_{\text{ext}} \rangle \\ = i \int d^3\mathbf{y} \langle V_0^c(y) \mathcal{O}_{\text{ext}} \rangle \end{aligned} \quad (2.2)$$

with $x_0 > y_0$ defining the hyperplanes.

We evaluate this identity on a lattice with Schrödinger functional boundary conditions (periodic in space, Dirichlet in time) [15, 16] with vanishing background field. The source operator \mathcal{O}_{ext} is built from the quark fields ζ and ζ' at the boundaries $x_0 = 0$ and $x_0 = T$:

$$\mathcal{O}_{\text{ext}} = -\frac{1}{6L^6} \epsilon^{cde} \mathcal{O}'^d \mathcal{O}^e \quad (2.3)$$

with

$$\mathcal{O}^e = a^6 \sum_{\mathbf{u}, \mathbf{v}} \bar{\zeta}(\mathbf{u}) \gamma_5 \frac{\tau^e}{2} \omega(\mathbf{u} - \mathbf{v}) \zeta(\mathbf{v}) \quad \text{and} \quad \mathcal{O}'^d = a^6 \sum_{\mathbf{u}, \mathbf{v}} \bar{\zeta}'(\mathbf{u}) \gamma_5 \frac{\tau^e}{2} \omega(\mathbf{u} - \mathbf{v}) \zeta'(\mathbf{v}), \quad (2.4)$$

where the wavefunction ω is understood to be an approximation of the pseudoscalar ground state. Its construction is detailed in [13, 14]. We summarize the results in section 4. The free index c that appears in eq. (2.3) is contracted with the free index from eq. (2.2). In this case, the term on the right-hand side involving the vector current can be simplified to the boundary-to-boundary correlator

$$F_1 = -\frac{1}{3L^6} \langle \mathcal{O}'^a \mathcal{O}^a \rangle \quad (2.5)$$

up to $O(a^2)$, as was shown in [10, 8] by using isospin symmetry.

In the remaining two terms on the left-hand side, the continuum currents are replaced by their improved and renormalized counterparts from the lattice. The result can be put in this form,

$$Z_A^2 (1 + b_A am_q)^2 [F_{AA}^I(x_0, y_0) - 2m \cdot F_{PA}^I(x_0, y_0)] = F_1, \quad (2.6)$$

with the improved correlation functions

$$\begin{aligned} F_{AA}^I(x_0, y_0) &= F_{AA}(x_0, y_0) + ac_A \left[\tilde{\partial}_{x_0} F_{PA}(x_0, y_0) + \tilde{\partial}_{y_0} F_{AP}(x_0, y_0) \right] \\ &\quad + a^2 c_A^2 \tilde{\partial}_{x_0} \tilde{\partial}_{y_0} F_{PP}(x_0, y_0), \end{aligned} \quad (2.7)$$

and

$$\tilde{F}_{PA}^I(x_0, y_0) = a \sum_{x'_0=y_0}^{x_0} w(x'_0) [F_{PA}(x_0, y_0) + ac_A \partial_{y_0} F_{PP}(x_0, y_0)], \quad (2.8)$$

where $\tilde{\partial}$ denotes the central difference operator and $F_{XY}(x_0, y_0)$ with $X, Y \in \{A, P\}$ stands for

$$F_{XY}(x_0, y_0) = -\frac{a^6}{6L^6} \sum_{\mathbf{x}, \mathbf{y}} \varepsilon^{abc} \varepsilon^{cde} \left\langle \mathcal{O}'^d X^a(x) Y^b(y) \mathcal{O}^e \right\rangle \quad (2.9)$$

and

$$w(x'_0) = \begin{cases} 1/2 & \text{if } x'_0 = y_0 \text{ or } x'_0 = x_0 \\ 1 & \text{if } y_0 < x'_0 < x_0 \end{cases} \quad (2.10)$$

implements the trapezoidal rule. Note that in eq. (2.6) the renormalization factors, which would arise from the boundary fields ζ and ζ' , cancel on both sides and that the product mP^a can be renormalized with the same factor Z_A as the axial current due to the PCAC relation. The mass-dependent term proportional to b_A will be dropped from here on, since we will impose the renormalization condition at vanishing mass. Of course, we can not tune the parameter to get exactly zero mass, but this only amounts to an $O(am)$ effect. Thus, our final renormalization condition is

$$Z_A = \lim_{m \rightarrow 0} \left[\frac{F_1}{F_{AA}^I(x_0, y_0) - 2m \cdot F_{PA}^I(x_0, y_0)} \right]^{\frac{1}{2}}. \quad (2.11)$$

In order to maximize the distance between the insertion points, we choose $x_0 = \frac{2}{3}T$ and $y_0 = \frac{1}{3}T$.

Except for F_1 , eq. (2.11) is built from correlators of the form given in eq. (2.9). When one evaluates these by performing the Wick contractions, one finds that only six contractions contribute, which are illustrated in figure 1. Two of them are disconnected. As argued in [8], they only give rise to $O(a^2)$ contributions and cancel in the continuum limit. By omitting them and taking only the connected contractions, one obtains an alternative renormalization condition. We will denote the corresponding renormalization factor by Z_A^{con} .

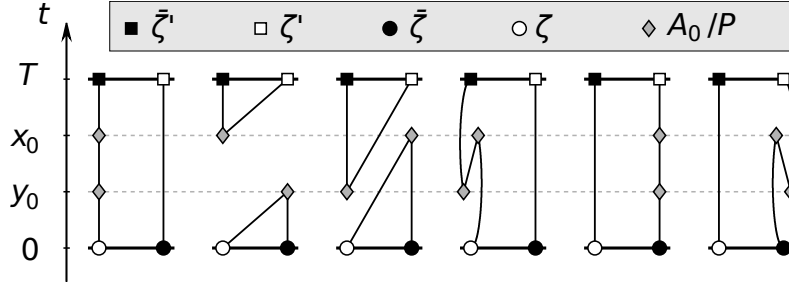


Figure 1: The six non-vanishing Wick contractions of correlation functions F_{XY} with source \mathcal{O}^{ext} and two bulk insertions X and Y , see eq. (2.9), taken from [8].

$L^3 \times T/a^4$	β	κ	#REP	#MDU	ID
$12^3 \times 17$	3.3	0.13652	10	10240	A1k1
		0.13660	10	13048	A1k2
$16^3 \times 23$	3.512	0.13700	2	20480	B1k1
		0.13703	1	8192	B1k2
		0.13710	3	24560	B1k3
$20^3 \times 29$	3.676	0.13700	4	15232	C1k2
		0.13719	4	15472	C1k3
$24^3 \times 35$	3.810	0.13712	7	15448	D1k1

Table 1: Overview of simulation parameters, number of replica and total number of molecular dynamics units of gauge configuration ensembles labeled by ‘ID’.

3. Simulations

To determine the renormalization factor Z_A of the axial current, we re-use the ensembles that were generated to obtain the improvement coefficient c_A .¹ These had already been designed to fit this purpose, in particular the ratio of the spatial and temporal extents was approximately $T/L \approx 3/2$ with $L \approx 1.2\text{fm}$. From [18], we expect this to be a good trade-off between a large infrared cutoff and small $\mathcal{O}(a^2)$ effects. An overview of the simulation parameters is given in table 1.

The coupling β was chosen such that the physical lattice size L stays roughly constant (line of constant physics). In this way, $\mathcal{O}(a^2)$ ambiguities in Z_A are guaranteed to smoothly vanish in the continuum limit. This was done using the perturbative relation between the lattice spacing a and the bare coupling. However, only the first two, universal coefficients b_0 and b_1 of the beta-function could be taken into account, because higher-order terms are not known for the TLI gauge action. To test for deviations from the line of constant physics, the gradient (or Wilson) flow coupling \bar{g}_{GF} was computed [19]. It is a renormalized coupling that depends on L as a scale, i.e., it will be constant if L is constant.

The parameter κ was tuned towards a vanishing PCAC mass. In [11], an upper bound of

¹The ensembles were generated using the openQCD code [17], see also <http://luscher.web.cern.ch/luscher/openQCD/>.

$|am_{\text{PCAC}}| < 0.015$ was employed. We expect that Z_A is more sensitive to the mass. Since at most values of β we have several ensembles with different κ values, we can check its influence explicitly by comparing the results.

In order to monitor the autocorrelation of the generated gauge configurations, several observables were computed alongside which are defined in terms of the gauge field smoothed by means of the gradient flow [20, 21]. Mostly, they showed autocorrelation times that did not exceed 250 MDU, only the topological charge became frozen at the largest $\beta = 3.810$. For c_A and Z_A , this should amount to a cutoff effect, but we have estimated it explicitly for c_A and have indeed found no significant deviations [13]. Further details, in particular about the algorithmic details can be also found in that reference.

4. Results

We have measured the correlators that are necessary to compute the renormalization factor and the PCAC mass on every second trajectory (in A1k2, A2k1) or every fourth trajectory (in the remaining ensembles). Via eq. (2.11), we compute Z_A as well as the alternative Z_A^{con} , where only the connected Wick contractions are included.

As already anticipated in eq. (2.4), our Schrödinger functional correlators involve boundary operators with a particular choice of wavefunction, which is constructed in such a way that it suppresses the contribution of the first excited state in the pseudoscalar channel. This optimal wavefunction was determined in the context of our non-perturbative calculation of the improvement coefficient c_A in [13] (see also [14] for a preliminary report), which employs the same gauge field ensembles at constant physics and the same kinematical setup as used here. It relies on demanding the quark mass extracted from the PCAC Ward identity to stay unchanged when the external states are varied, where in practice these external states are modeled as superpositions of spatial trial (hydrogen-like) wavefunctions designed to approximately maximize the overlap with the ground and first excited state, respectively. For the purpose of Z_A , however, only the wavefunction for the approximate pseudoscalar ground state is required, which we therefore choose as the one already obtained in [13], i.e.,

$$\omega_{\pi^{(0)}} = \sum_{i=1}^3 \eta_i^{(0)} \omega_i, \quad \eta^{(0)} = (0.5317, 0.5977, 0.6000), \quad (4.1)$$

in terms of the basis of suitable trial wavefunctions ω_i mentioned above. With this wave function at hand, the eq. (2.11) for Z_A is evaluated upon prior projection of all entering correlation functions to this approximate ground state.

Moreover, as it is evident from eqs. (2.7) and (2.8), a genuine non-perturbative determination of Z_A also requires the knowledge of non-perturbative values for c_A for our simulation parameters. We thus rely on the result of our aforementioned recent non-perturbative computation of c_A in three-flavor lattice QCD with tree-level improved gauge action [13], which we reproduce here for convenience:

$$c_A(g_0^2) = -0.006033 g_0^2 \times [1 + \exp(9.2056 - 13.9847 \cdot g_0^{-2})]; \quad (4.2)$$

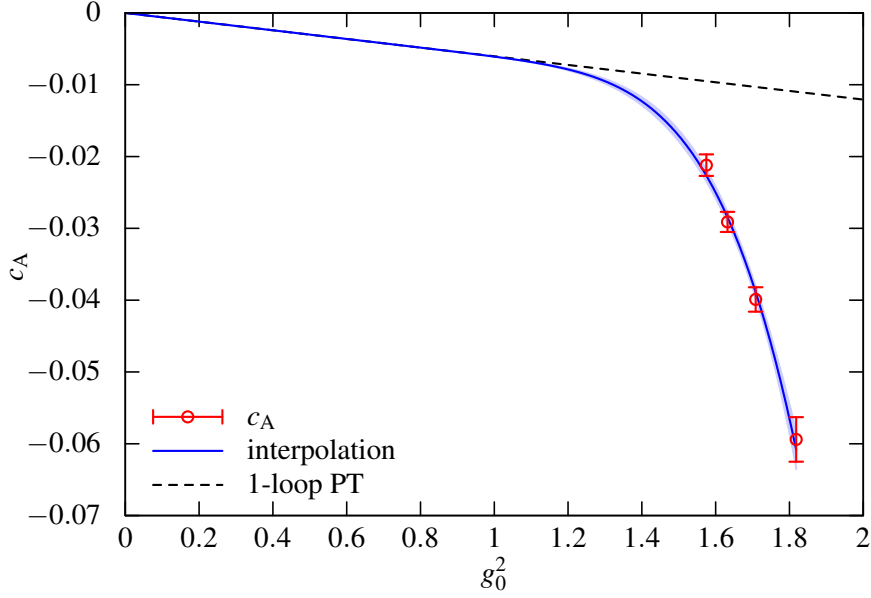


Figure 2: Final results for c_A together with interpolation [13]. The dotted line indicates the perturbative 1-loop asymptotics [22].

this formula is valid for bare couplings below $g_0^2 \approx 1.8$ and with statistical errors between $\approx 4\%$ near the largest and $\approx 8\%$ near the smallest bare couplings simulated. For further details about this determination of c_A we refer to refs. [13, 14].

Our preliminary results for Z_A obtained for the ensembles considered so far are collected in table 2. In our tentative error analysis, we estimate the errors on Z_A for each replicum via a full autocorrelation analysis as described in [23] and compute a weighted average over all replica within an ensemble.

Table 2 also includes the unrenormalized PCAC mass am_{PCAC} , which is computed using the perturbative value of c_A and the wavefunction $\omega_{\pi(0)}$, the gradient-flow coupling \bar{g}_{GF}^2 and the results for Z_A^{con} obtained via the alternative definition of the renormalization factor, which includes only connected contractions.

As can be seen from the table, \bar{g}_{GF}^2 is approximately constant, only the deviation on the ensemble D1k1 at the largest β is more pronounced. We do not expect that this deviation from constant physics has a significant effect on our result, but we plan to check it explicitly using the ensemble B2k1 from [13], whose parameters are identical to the ones of B1k1 except for β . Some of the ensembles in the B and C groups show a significant though not yet severe mass dependence. We consider taking a closer look at this issue and adding new ensembles with different κ values, too.

For $L/a = 12$ ($\beta = 3.3$), Z_A^{con} differs significantly from the standard value Z_A , which seems to signal significant $O(a^2)$ uncertainties in Z_A at this lattice spacing ($a \approx 0.09$ fm). Similarly large cutoff effects at this β were also observed for this action in [24]. However, at smaller lattice spacings the results for both definitions of Z_A are in good agreement within their errors. We plan to examine the impact of cutoff effects on Z_A more closely by adding an ensemble at $L/a = 14$ ($\beta = 3.414$).

ID	am_{PCAC}	\bar{g}_{GF}^2	Z_A^{con}	Z_A	
A1k1	−0.0010(7)	18.12(21)	0.8162(78)	0.6553(90)	*
A1k2	−0.0086(6)	16.95(13)	0.8290(92)	0.6489(72)	
B1k1	+0.0063(2)	16.49(13)	0.7757(23)	0.7666(47)	
B1k2	+0.0056(3)	16.85(20)	0.7758(45)	0.7677(71)	
B1k3	+0.0022(2)	16.11(14)	0.7804(30)	0.7516(36)	*
C1k2	+0.0066(2)	15.53(14)	0.7889(16)	0.7888(48)	
C1k3	−0.0005(1)	14.64(13)	0.7822(27)	0.7785(33)	*
D1k1	−0.00269(8)	13.90(11)	0.7969(16)	0.7904(16)	*

Table 2: Summary of results: the unrenormalized PCAC quark mass, the gradient-flow coupling, the results for Z_A using the alternative definition (Z_A^{con}) and the standard definition including disconnected contractions. Ensembles marked by ‘*’ are used in the fit procedure.

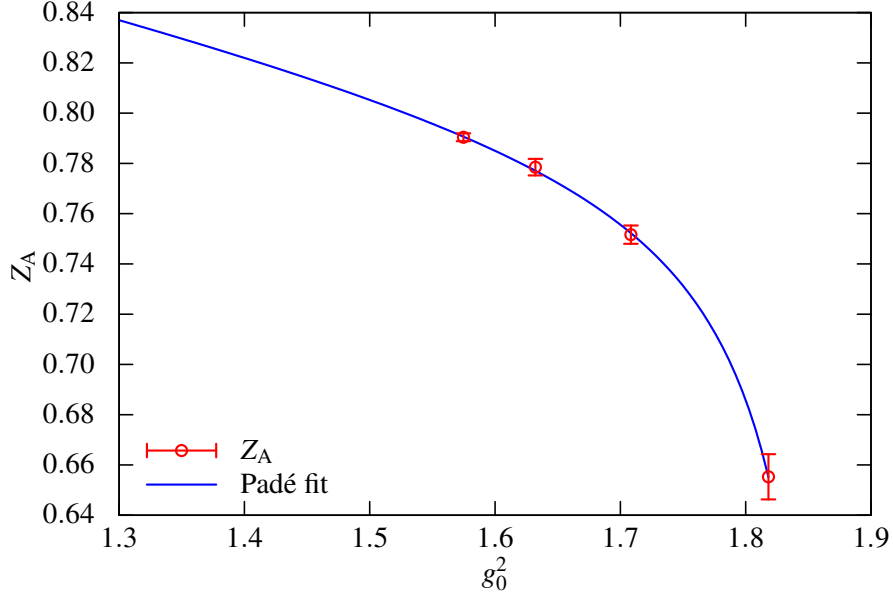


Figure 3: Plot of our preliminary estimate of Z_A versus the bare coupling g_0^2 . The data points and a Padé fit are shown.

In figure 3, the Z_A values of the four ensembles with the smallest absolute PCAC mass at each value of β are plotted against the bare coupling. They have been used to determine a Padé approximation of $Z_A(g_0^2)$ based on the ansatz

$$Z_A(g_0^2) = \frac{1 + a_1 \cdot g_0^2 + a_2 \cdot g_0^4}{1 + b_1 \cdot g_0^2}, \quad (4.3)$$

which is constrained to yield the correct continuum limit $Z_A(0) = 1$. The coefficients we found are

$$a_1 = -0.6492, \quad a_2 = 0.0619, \quad b_1 = -0.5298. \quad (4.4)$$

With these parameters, the fit function lies well within the errors of all data points.

Let us emphasize again that the results on Z_A should be regarded as preliminary, since a final error analysis as well as the inclusion of the reweighting factors (to compensate for the approximation errors of the RHMC algorithm employed for the third quark in our simulations) are still missing. Regarding the latter, our experience from c_A leads us to expect only a minor influence from them. Moreover, to account for the topology freezing observed at the finest lattice spacing, we will supplement our definition of Z_A with the condition to restrict the analysis to the sector of zero topological charge, as we did for c_A [13].

5. Conclusions

We have determined a preliminary expression for the renormalization factor $Z_A(g_0^2)$ of the isovector axial current for the tree-level improved gauge action and three dynamical flavors of Wilson fermions. It is summarized in the interpolation formula of eq. (4.3). Together with the improvement coefficient c_A , which has already been determined non-perturbatively [13], this will make it possible to obtain precise results for matrix elements such as pseudoscalar decay constants. However, before our result is applied, we will scrutinize our analysis by projection to the zero-topology sector and also investigate deviations from the constant physics condition. In addition, a simulation at another point ($L/a = 14$, $\beta = 3.414$) along our line of constant physics is under way to shed light on the cutoff effects reflected at the coarsest lattice spacing by the differences between Z_A and Z_A^{con} .

Acknowledgments We want to thank R. Hoffmann, P. Fritzsch and S. Takeda, who are the original authors of the script that we used in parts of our analysis. We are indebted to Rainer Sommer and Stefan Schaefer for helpful advice as well as Alberto Ramos, who additionally provided us with his analysis program measuring the gradient-flow coupling. This work is supported by the grant HE 4517/3-1 (J. H. and C. W.) of the Deutsche Forschungsgemeinschaft. We gratefully acknowledge the computing time granted by the John von Neumann Institute for Computing (NIC) and provided on the supercomputer JUROPA at Jülich Supercomputing Centre (JSC). Computer resources were also provided by DESY, Zeuthen (PAX Cluster), the CERN thqcd2 installation, and the ZIV of the University of Münster (PALMA HPC cluster).

References

- [1] K. G. Wilson, *Phys. Rev.* **D10** (1974) 2445.
- [2] B. Sheikholeslami and R. Wohlert, *Nucl. Phys.* **B259** (1985) 572.
- [3] K. Symanzik, *Nucl. Phys.* **B226** (1983) 187.
- [4] K. Symanzik, *Nucl. Phys.* **B226** (1983) 205.
- [5] P. Fritzsch, F. Knechtli, B. Leder, M. Marinkovic, S. Schaefer, et al., *Nucl. Phys.* **B865** (2012) 397 [[arXiv:1205.5380](#)].
- [6] M. Della Morte, R. Hoffmann, and R. Sommer, *JHEP* **03** (2005) 029 [[hep-lat/0503003](#)].
- [7] T. Kaneko et al., *JHEP* **0704** (2007) 092 [[hep-lat/0703006](#)].

- [8] M. Della Morte, R. Hoffmann, F. Knechtli, R. Sommer, and U. Wolff, *JHEP* **07** (2005) 007 [[hep-lat/0505026](#)].
- [9] M. Lüscher, S. Sint, R. Sommer, P. Weisz, and U. Wolff, *Nucl. Phys.* **B491** (1997) 323 [[hep-lat/9609035](#)].
- [10] M. Lüscher, S. Sint, R. Sommer, and H. Wittig, *Nucl. Phys.* **B491** (1997) 344 [[hep-lat/9611015](#)].
- [11] J. Bulava and S. Schaefer, *Nucl. Phys.* **B874** (2013) 188 [[arXiv:1304.7093](#)].
- [12] M. Lüscher and P. Weisz, *Commun. Math. Phys.* **97** (1985) 59.
- [13] J. Bulava, M. Della Morte, J. Heitger, and C. Wittemeier [[arXiv:1502.04999](#)].
- [14] J. Bulava, M. Della Morte, J. Heitger, and C. Wittemeier, *PoS LATTICE2013* (2014) 311 [[arXiv:1312.3591](#)].
- [15] M. Lüscher, R. Narayanan, P. Weisz, and U. Wolff, *Nucl. Phys.* **B384** (1992) 168 [[hep-lat/9207009](#)].
- [16] S. Sint, *Nucl. Phys.* **B421** (1994) 135 [[hep-lat/9312079](#)].
- [17] M. Lüscher and S. Schaefer, *Comput. Phys. Commun.* **184** (2013) 519 [[arXiv:1206.2809](#)].
- [18] M. Della Morte, R. Sommer, and S. Takeda, *Phys. Lett.* **B672** (2009) 407 [[arXiv:0807.1120](#)].
- [19] P. Fritzsche and A. Ramos, *JHEP* **1310** (2013) 008 [[arXiv:1301.4388](#)].
- [20] M. Lüscher, *JHEP* **1008** (2010) 071 [[arXiv:1006.4518](#)].
- [21] M. Lüscher and P. Weisz, *JHEP* **1102** (2011) 051 [[arXiv:1101.0963](#)].
- [22] S. Aoki, R. Frezzotti, and P. Weisz, *Nucl. Phys.* **B540** (1999) 501 [[hep-lat/9808007](#)].
- [23] U. Wolff, *Comput. Phys. Commun.* **156** (2004) 143 [[hep-lat/0306017](#)].
- [24] M. Bruno, D. Djukanovic, G. P. Engel, A. Francis, G. Herdoiza, et al., *JHEP* **1502** (2015) 043 [[arXiv:1411.3982](#)].